

See discussions, stats, and author profiles for this publication at: <https://www.researchgate.net/publication/43652119>

Interaction between Charged Surfaces on the Poisson–Boltzmann Level: The Constant Regulation Approximation

ARTICLE *in* THE JOURNAL OF PHYSICAL CHEMISTRY B · DECEMBER 2004

Impact Factor: 3.3 · DOI: 10.1021/jp0473063 · Source: OAI

CITATIONS

52

READS

52

4 AUTHORS:



Ramon Pericet-Camara

École Polytechnique Fédérale de Lausanne

24 PUBLICATIONS 451 CITATIONS

SEE PROFILE



Georg Papastavrou

University of Bayreuth

53 PUBLICATIONS 1,241 CITATIONS

SEE PROFILE



Sven Holger Behrens

Georgia Institute of Technology

75 PUBLICATIONS 2,003 CITATIONS

SEE PROFILE



Michal Borkovec

University of Geneva

234 PUBLICATIONS 12,830 CITATIONS

SEE PROFILE

Interaction between Charged Surfaces on the Poisson–Boltzmann Level: The Constant Regulation Approximation

Ramon Pericet-Camara,[†] Georg Papastavrou,[‡] Sven H. Behrens,[‡] and Michal Borkovec^{*,†}

Department of Inorganic, Analytical, and Applied Chemistry, University of Geneva, 30 Quai Ernest-Ansermet, 1211 Geneva 4, Switzerland, and Polymer Research Laboratory, BASF Aktiengesellschaft, Ludwigshafen, Germany

Received: June 21, 2004; In Final Form: September 29, 2004

Interaction forces between ionizable surfaces across an electrolyte solution on the Poisson–Boltzmann level are discussed within the constant regulation approximation. The chemical response of each surface is expressed in terms of two parameters, namely, the diffuse layer potential and the regulation parameter p . Both parameters are easily available because they arise naturally within classical equilibrium models for a single noninteracting surface. This approximation, thus, eliminates the need to treat the more intricate problem of two chemical adsorption equilibria coupled to the overlapping double layers between the surfaces. The ensuing simplicity makes this approach extremely versatile for the analysis of experimental data. The classical boundary condition of constant potential corresponds to $p = 0$, and that of constant charge corresponds to $p = 1$. While this approximation is rigorously correct at large separations, we find that it remains excellent down to contact in many realistic situations, such as in symmetric or asymmetric systems involving metal oxides or silica described by the 1-pK basic Stern model.

1. Introduction

In recent years, one could witness substantial progress in the measurement of interaction forces between surfaces, particularly with the surface forces apparatus,^{1–5} colloidal probe technique,^{6–12} or total internal reflection microscopy.^{13,14} The interaction force as a function of the separation distance is of major interest in aqueous media, most notably because of their importance in biological systems, mineral processing, and the natural environment.^{15–17} Surfaces of solids in contact with water are charged, and, therefore, interactions between such surfaces are typically dominated by electrostatic forces, originating from the overlap of the electric double layers. By superposing such electrostatic forces with van der Waals interactions, one adopts the assumption of the famous theory of Derjaguin, Landau, Verwey, and Overbeek (DLVO).^{18,19} While this assumption has been challenged recently,²⁰ direct force measurements repeatedly confirmed the relevance of electrostatic and dispersion forces in real systems.^{1,2,6,9–11} In many situations, the DLVO theory, thus, provides a quantitative description of the interaction force down to separations of a few nanometers.

The electrostatic forces are typically treated on the Poisson–Boltzmann (PB) level, which invokes a mean-field approximation for the electrolyte solution.¹ The PB approximation remains accurate for monovalent aqueous electrolytes up to concentrations of about 0.1 M and surface charge densities of approximately 0.2 C m^{−2}, as confirmed with studies of the primitive model.^{21–24} The solution of the PB equation requires a choice of boundary conditions, and usually either the constant charge (CC) or the constant potential (CP) boundary condition is used. The CC condition assumes that the diffuse layer charges

remain constant as the surfaces approach each other, while the surface potential changes according to the charge–potential relationship of the diffuse layer, as defined by the PB equation. The assumption of CC can be realistic for systems where the surface charge originates either from strong acid or base groups (e.g., sulfate or amidine latex), from isotopic substitution of minerals (e.g., mica), or in the case of kinetic limitations during rapid approach of the surfaces.^{1,25,26} The CP condition assumes a constant surface potential during approach, which is accompanied by a change of the surface charge. For an electrode surface, CP could be maintained by a potentiostat.^{4,27,28} As shown recently and reiterated below, the CP condition is also a good approximation for metal oxide surfaces at low ionic strengths and near its point of zero charge (PZC).³¹ The solution of the PB equation can be found numerically or obtained on the basis of the analytical solution in terms of elliptic functions.^{16,26,29–36}

Inspection of available direct force measurements reveals that normally neither the CC nor the CP condition represents a good approximation.^{1,2,6,9–11} The measured forces typically lie between these two cases, a situation which is referred to as charge regulation.^{1,16,17,31–33} In this situation neither the diffuse layer charge nor the diffuse layer potential remain constant, but both quantities vary with the separation as a result of an interplay between the charge–potential relationships of the diffuse layer and of the surface. The charge–potential relationship of the surface reflects how the surface charge varies as a function of the diffuse layer potential and is dictated by the dissociation reactions occurring at the surface (i.e., surface complexation).^{38–41}

Charge regulation has been treated by several authors employing detailed models of the dissociation behavior of the surface.^{30–36} From these theoretical studies it becomes clear that consideration of the charge regulation normally leads to results between the case of CC and the case of CP, and calculated force–distance curves do resemble the experimental results.

* Corresponding author. Phone: +41 22 379 6405. Fax: +41 22 379 6069. E-mail: michal.borkovec@unige.ch. Web: <http://colloid.unige.ch/>.

[†] University of Geneva.

[‡] BASF Aktiengesellschaft.

Unfortunately, however, such calculations are cumbersome, highly model-dependent, and for this reason of limited practical use for routine data analysis. On the basis of these studies one might in fact suspect that without detailed models of the surface dissociation behavior, no calculations of the regulation behavior are possible. The resulting restriction would be severe, because for many systems of interest accurate surface charging models are not available (e.g., adsorbed polyelectrolytes).

Carnie and Chan³⁷ were the first to suggest how to circumvent this dilemma by considering a regulation parameter interpolating between the CC and the CP cases. This parameter was defined in terms of the diffuse layer capacitance C^D and a regulation capacitance C^I , both capacitances referring to the charge–potential relationships of the diffuse layer and of the surface, respectively. Both relationships have been linearized, and, consequently, the diffuse layer was treated within the Debye–Hückel approximation. The latter approximation is rather restrictive, however, because it linearizes the PB equation and is, therefore, applicable up to surface potentials of only 20–30 mV. For this reason, many realistic systems fall outside the range of this approximation.

More recently, it has been shown that the regulation parameter can be generalized to the PB level.^{31,32} This parameter p can be obtained from the capacitances of the diffuse and the surface layer and typically assumes the values $0 < p < 1$, with $p = 0$ for CP and $p = 1$ for CC. In the symmetric situation, an approximate scheme was further proposed to construct the force–distance curves from this regulation parameter and the CP and CC force profiles.³² Nevertheless, the utility of the regulation parameter to calculate force–distance curves in the asymmetric PB case remained unclear.

The present article shows how the regulation parameter p can be used to define a constant regulation (CR) boundary condition in the nonlinear PB regime. With this boundary condition one can treat symmetric and asymmetric situations in the PB regime to excellent accuracy. The spirit of this approximation is that the diffuse layer is treated exactly within the PB equation, while the charge–potential relationship of the surface is linearized around the potential of the isolated surface. This approximation characterizes each surface with two parameters, namely, the diffuse layer potential $\psi^{D,\infty}$ and the regulation parameter p . The key advantage of this approximation is that these two parameters suffice to approximate the detailed charge–potential relationship. This parametrization is completely generic and entirely independent of the molecular details of reactions occurring on each particular surface. Both parameters can be extracted from experimental force–distance curves or derived from models for dissociation equilibria for the isolated surface. Within this article, we shall demonstrate the high accuracy of the CR approximation by comparing the corresponding results with an exact treatment of the surface dissociation equilibria for realistic systems. The comparison with experimental data is beyond the scope of the present paper and will be discussed elsewhere.

2. Interaction Forces on the PB Level

We consider two charged, parallel plane surfaces immersed in a monovalent electrolyte solution separated by a distance L . The spatial coordinate normal to the surface will be denoted by x , and the position of the surface 1 (left) will be chosen at $x = 0$ and of the surface 2 (right) at $x = L$. The charges on the surface will create a diffuse layer in their vicinity. These diffuse layers overlap for small separations between the surfaces. The properties of these diffuse layers are determined by the dissociation equilibria at both surfaces.

Diffuse Layer Profile. The electrostatic potential $\psi(x)$ within the diffuse layer is described with the PB equation (eq 1)

$$\frac{d^2\psi}{dx^2} = \frac{\kappa^2}{\beta e} \sinh(\beta e \psi) \quad (1)$$

where e is the elementary charge, $\beta = 1/(kT)$ is the inverse thermal energy, and κ^{-1} is the Debye length defined by $\kappa^2 = 2\beta e^2 n / (\epsilon \epsilon_0)$, whereby n is the number concentration of the monovalent salt in the bulk and $\epsilon \epsilon_0$ is the dielectric permittivity of water. At the boundaries, the potential profile satisfies

$$\psi_1^D = \psi(0) \quad (2)$$

$$\psi_2^D = \psi(L) \quad (3)$$

where the ψ_1^D and ψ_2^D are the diffuse layer potential of the surfaces 1 and 2, respectively. Fixing these two parameters leads to the CP boundary conditions. Furthermore,

$$\sigma_1^D = -\epsilon \epsilon_0 \left. \frac{d\psi}{dx} \right|_{x=0} \quad (4)$$

$$\sigma_2^D = \epsilon \epsilon_0 \left. \frac{d\psi}{dx} \right|_{x=L} \quad (5)$$

where the σ_1^D and σ_2^D are the diffuse layer charge densities of the surfaces 1 and 2, respectively. Fixing these two parameters leads to the CC boundary conditions.

In the general case, neither the CC nor the CP boundary conditions represent a good approximation, and one must use an explicit model of surface dissociation equilibria and derive a charge–potential relationship for the inner (compact) layer of each surface. This charge corresponds to the total charge on the surface and will be a function of the diffuse layer potential. Let us denote these relations for both surfaces as $\sigma_1^I(\psi_1^D)$ and $\sigma_2^I(\psi_2^D)$. Note that these relations only depend on the properties of the surface but not on the surface separation L . The above system of equations can be closed by realizing that the diffuse layer charge must be neutralized by the inner layer charge, namely,

$$\sigma_1^D = \sigma_1^I(\psi_1^D) \quad (6)$$

$$\sigma_2^D = \sigma_2^I(\psi_2^D) \quad (7)$$

These relations complete the system of equations, and eqs 1–7 can be solved. Several authors have proposed solutions in terms of elliptic functions.^{30,32,33,35,36} However, we find a direct numerical solution of the PB equation with a deferred correction technique and Newton iteration equally accurate, efficient, and much easier to implement in the asymmetric case.⁴²

At large separation distances, the diffuse layer charge is given by the Grahame equation

$$\sigma^D = \frac{2\epsilon \epsilon_0 \kappa}{\beta e} \sinh(\beta e \psi^D / 2) \quad \text{for } L \rightarrow \infty \quad (8)$$

while the diffuse layer capacitance is given by its derivative

$$C^D = \frac{\partial \sigma^D}{\partial \psi^D} = \epsilon \epsilon_0 \kappa \cosh(\beta e \psi^D / 2) \quad (9)$$

The solution of eqs 6 and 7 yields the surface potentials for each isolated surface, denoted as $\psi_1^{D,\infty}$ and $\psi_2^{D,\infty}$. Equivalently,

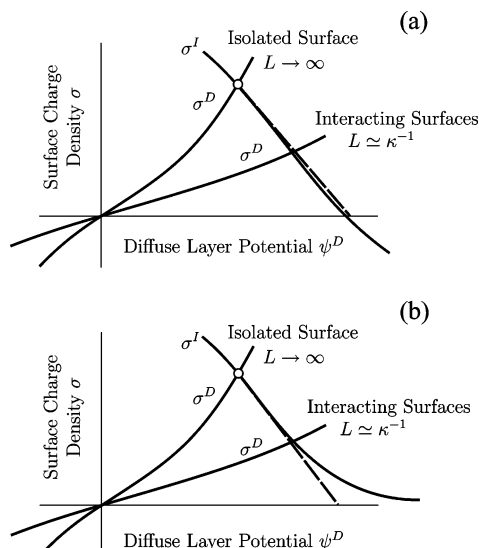


Figure 1. Schematic representation of the charge–potential relationships for two equal interacting surfaces. The inner layer charge density σ^I typically decreases with increasing double layer potential. It is independent of the surface separation L but depends on the surface chemistry. The diffuse layer charge density σ^D increases with increasing double layer potential. It depends on the separation L but is independent of the surface properties. For an isolated surface this relation is given by the Grahame equation (cf. eq 8). The magnitude of σ^D decreases with decreasing separation L , and it vanishes at contact. The equilibrium point is given by $\sigma^I = \sigma^D$ at any separation and is marked for the isolated surface (○). The dashed line is the CR approximation for the inner layer charge density σ^I . The approximation works well even down to contact for part a but fails near contact for part b.

one may also specify the diffuse layer charge of the isolated surface, $\sigma_1^{D,\infty}$ and $\sigma_2^{D,\infty}$. Both quantities are often loosely referred to as the “diffuse layer potential” and “diffuse layer surface charge”, although they refer to infinite separation. At finite separations, the potential and charge of the diffuse layer vary as a function of the distance.

Figure 1 illustrates the situation for a symmetric system. The diffuse layer charge σ^D increases with the surface potential, while the inner layer charge σ^I typically is a decreasing function. The crossing point of these two functions defines the surface potential. With decreasing distance between the plates, surface charge normally decreases, and the crossing point shifts to higher surface potentials.

CR Boundary Condition. Let us now discuss the charging properties of the compact layer in more detail. For clarity, we shall drop the subscript referring to the surface 1 or 2. The compact layer capacitance can be defined as

$$C^I = -\frac{\partial \sigma^I}{\partial \psi^D} \quad \text{for } L \rightarrow \infty \quad (10)$$

At large separations we may expand the charge–potential relationships around the potential at infinite separation in a Taylor series

$$\sigma^I = \sigma^{I,\infty} - C^I(\psi^D - \psi^{D,\infty}) \quad (11)$$

and replace the charge–potential relationship of the inner layer by a straight line (see Figure 1, dashed line). In a first approximation, each surface can be characterized by the diffuse layer potential $\psi^{D,\infty}$ and the inner layer (regulation) capacitance C^I , both quantities being evaluated for the isolated surface. The inner layer capacitance describes the regulation characteristics of the surface, whereby a small capacitance corresponds to the

CC case, while a large (positive) capacitance corresponds to the CP case. Because the regulation capacitance C^I used in the charge–potential relationship is a constant, we will be employing the term *constant regulation*. Instead of this capacitance, we prefer to introduce the regulation parameter^{31,32}

$$p = \frac{C^D}{C^I + C^D} \quad (12)$$

to characterize the regulation properties of each surface. Applying eq 11 to each surface, we obtain a closed system of equations, and this approximation will be referred to as the CR boundary condition.

The substantial advantage of the above formulation is that the regulation characteristics of each surface are contained in merely two quantities, namely, the diffuse layer potential $\psi^{D,\infty}$ and the regulation parameter p , both being properties of an isolated surface. The quality of the approximation can be deduced from Figure 1. This approximation is asymptotically exact for large distances, even at large surface potentials. The latter aspect makes the present CR approximation much more versatile than the approach of Carnie and Chan,³⁷ which is only applicable at low surface potentials.

The performance of the CR approximation near contact is not obvious, but its validity can be assessed by considering the charge–potential relationship for the inner layer. Naturally, when this relationship is close to a linear function, the approximation will be excellent (see Figure 1a). This situation applies particularly for surfaces with a well-defined PZC, such as most metal oxides. On the other hand, if the curvature of the charge–potential relationship is large, the approximation may fail at short distances (see Figure 1b). This situation is commonly encountered for surfaces which become neutral upon full desorption or full saturation of the charge-determining ion. In this case, as σ^I tends toward 0, the magnitude of the surface potential increases dramatically. An important example of such a situation is silica. We shall see, however, that even for such a surface, the CR approximation remains excellent except for small separations.

Basic Stern Model. To investigate the quality of the proposed CR approximation, we shall use established models of surface dissociation equilibria for realistic systems and compare the exact results with the CR approximation.

The basic Stern model has been shown to be valid for a number of interfaces of metal oxides, and for that reason this model will be used in the following.^{40,41} This model considers a surface whose charge varies by means of the adsorption of protons to different surface sites. The mass action law for each type of site j can be written as

$$K_j = \frac{\theta_j}{(1 - \theta_j)a_H(0)} \quad (13)$$

where K_j is the microscopic association constant, θ_j is the degree of protonation, and the surface activity of protons is given by $a_H(0) = a_H \exp(-\beta e \psi^0)$ where ψ^0 is the surface potential and a_H is their bulk activity with $\text{pH} = -\log a_H$. The association constant is usually reported as $\text{p}K_j = \log K_j$. The surface charge can be then evaluated as

$$\sigma^I = e \sum_j \Gamma_j (\theta_j + z_j) \quad (14)$$

where z_j is the charge of the site j in its deprotonated state and Γ_j is its total site density. The diffuse layer potential is related

to the surface potential by the Stern capacitance, which is defined as

$$C^S = \frac{\sigma^I}{\psi^0 - \psi^D} \quad (15)$$

From eqs 13–15 the charge–potential relationship for the inner layer $\sigma^I(\psi^D)$ can be constructed. This nonlinear relationship can be then used to solve the PB equation. For large separations, the solution reduces to the classical solution of the basic Stern model for isolated surfaces, which invokes the Grahame equation (cf. eq 8). An equivalent approach was adopted earlier.^{31,33}

Interaction Forces. Once the potential profile is known, the force between two bodies can be evaluated from the pressure between the plates.¹ The pressure follows from

$$\Pi = 2nkT [\cosh(\beta e\psi) - 1] - \frac{\epsilon\epsilon_0(d\psi)^2}{2(dx)} \quad (16)$$

This expression is an invariant, meaning that it holds at any position x . This feature represents a useful check of the numerical accuracy of the solution.

Once the pressure is known, the surface free energy can be evaluated by integration of eq 16. On the basis of the Derjaguin approximation, the force between two bodies becomes

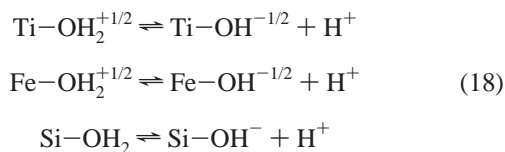
$$F = 2\pi R \int_L^\infty \Pi(L') dL' \quad (17)$$

where R is the mean curvature radius defined as $R^{-1} = R_1^{-1} + R_2^{-1}$ where R_1 and R_2 are the principal curvature radii of the respective surfaces. This integration is performed numerically. Equivalent procedures have been used by others.^{1,30}

3. Exemplary Oxide Surfaces

To illustrate the utility of the CR approximation, we shall present exact numerical solutions of the interaction forces on the PB level between different oxide surfaces. The charging behavior of these surfaces will be treated within a classical surface complexation model.^{38–41} We shall present a few results for symmetric systems but mostly focus on asymmetric systems. As we shall see, in the vast majority of the situations, the CR approximation is extremely accurate even down to contact.

Three oxide surfaces will be used to illustrate the rich behavior of the electrostatic forces, which may be encountered in asymmetric situations. The surfaces considered are rutile (TiO_2), goethite (FeOOH), and silica (SiO_2). The charging properties of the surfaces can be described by the 1-pK basic Stern model.^{40,41} The charging behavior will be modeled as originating from one surface group, namely, as



where we introduce for rutile and goethite the charge of $+1/2$ in the protonated state and $-1/2$ in the deprotonated state, while for the silica surface the silanol group is neutral when protonated and has a charge of -1 when deprotonated. Table 1 summarizes the relevant parameters used to describe these systems. In all three cases, this parametrization provides a rather accurate description of the overall charge of these oxides as determined by potentiometric titrations.^{40,41} As an alternative, various

TABLE 1: Parameters of the 1-pK Basic Stern Model for Oxide Surfaces

		pK	z	Γ (nm ⁻²)	C^S (F/m ²)
rutile	TiO ₂	5.8	-1/2	12.2	1.33
goethite	FeOOH	9.5	-1/2	6.15	1.10
silica	SiO ₂	7.5	-1	8.00	2.90

authors have used so-called 2-pK models, largely with equivalent results.^{38,39} Because of its simplicity, we focus on the 1-pK picture here.

The charging behavior of these three surfaces as a function of pH and for different ionic strengths is summarized in Figure 2. The columns refer to different oxides, while the rows refer to different surface properties. The top row shows the surface charge density, the middle row the diffuse layer potential, and the last row the regulation parameter. Note that all these properties are evaluated for an isolated surface.

Rutile and goethite are classical examples of amphoteric oxides, which are positively charged at low pH and negatively charged at high pH. At one particular pH value, the surface is uncharged, and one refers to the PZC. When the surface charge density is plotted as a function of pH for different ionic strengths, the PZC is immediately recognized as the common crossing point. The surface charge density depends more strongly on the pH for high ionic strength, while for low ionic strength its dependence is weaker.

The diffuse layer potentials decrease with increasing pH from positive to negative values and vanish at the PZC. The magnitude of the diffuse layer potential decreases with increasing ionic strength, as a result of more pronounced screening. At the same time, charging of the surface is facilitated by screening of the interactions between the sites. The combination of these two effects explains why the surface charge density and the diffuse layer potential show the opposite trends with the ionic strength.

For amphoteric oxides, the regulation parameter exhibits a minimum as a function of pH at the PZC. This minimum becomes more pronounced with decreasing ionic strength. Because the inner layer capacitance varies little near the PZC, this minimum reflects the dependence of the diffuse layer capacitance on the surface potential (cf. eq 9). The latter is lowest for a weakly charged surface and increases strongly with increasing magnitude of the surface potential. Furthermore, the diffuse layer capacitance increases with increasing ionic strength. The regulation parameter follows, therefore, the same trends. Recall that $p = 1$ corresponds to the CC boundary condition, while $p = 0$ corresponds to CP. We, thus, conclude that metal oxide surfaces near the PZC can be well approximated by CP boundary conditions, particularly at low ionic strengths. Further away from the PZC, however, their regulation behavior may be very different and eventually approaches CC conditions.

Silica behaves differently. The surface charge density vanishes at low pH and decreases with increasing pH. The behavior of the surface charge density and of the diffuse layer potential qualitatively resembles the discussed behavior of a metal oxide above the PZC. However, as a result of the low surface density of the charged groups at low pH, the surface charge density varies in this region only marginally. As a consequence, the diffuse layer capacitance also remains close to constant. The regulation parameter, thus, shows a minimum as a function of pH, but its values always remain relatively high. Silica will, therefore, rather resemble CC conditions. At very low pH, the neutral silanol groups start to protonate, and silica acquires a weakly positive charge.^{40,41} However, this effect is negligible in the situations discussed here and, therefore, not considered.

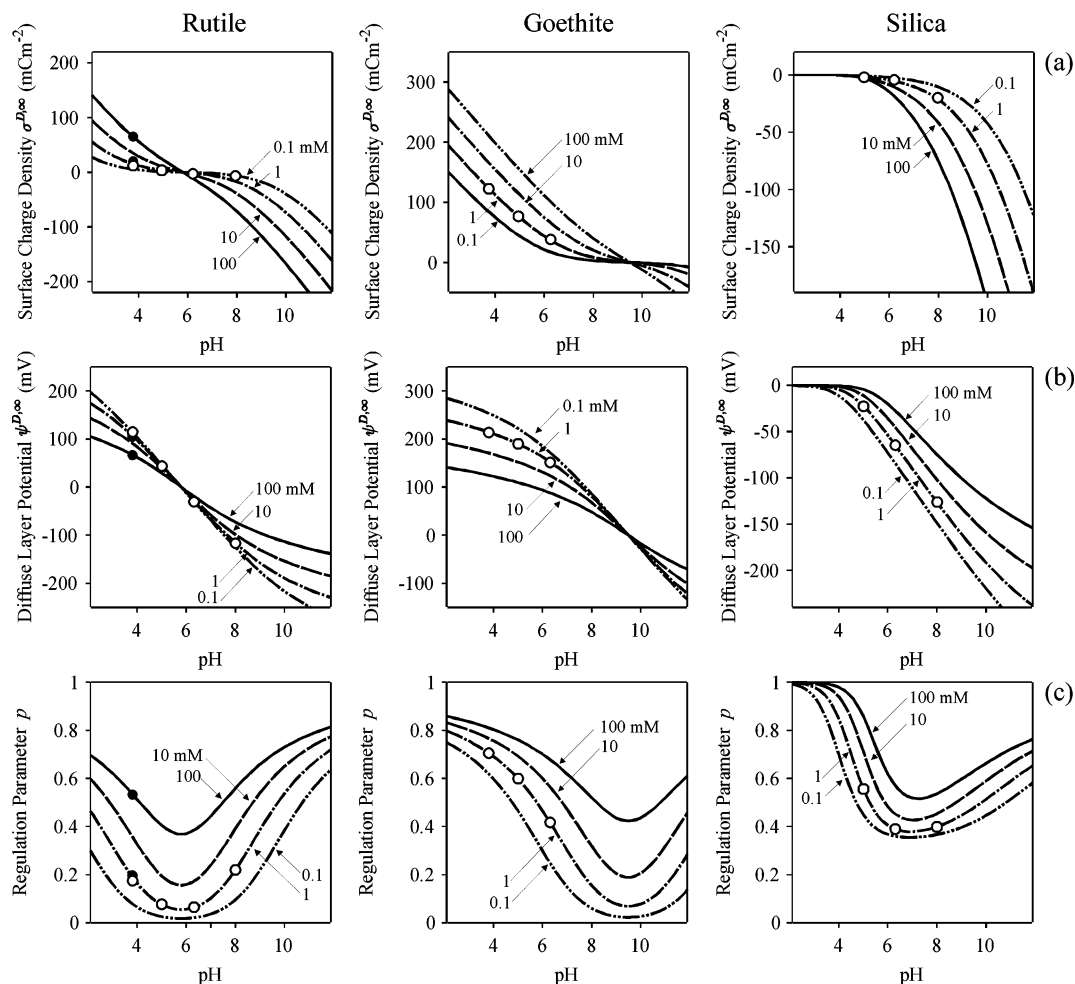


Figure 2. Charging behavior obtained from the basic Stern 1-pK model of three representative oxide surfaces, namely, rutile, goethite, and silica (from left to right). Various surface properties are represented for different ionic strengths as a function of pH. (a) Surface charge density, (b) diffuse layer potential, and (c) regulation parameter. The first two oxides show a PZC, while silica remains negative. The conditions used in the force calculations in symmetric (●) and asymmetric (○) cases are indicated.

The reason for the different behavior of the amphoteric oxide and silica surfaces at low charge densities originates from their different surface chemistries (see eq 18). For the oxide surface, there is a large number of ionized groups, bearing either a positive (protonated group) or a negative charge (deprotonated group). The adsorption of protons to such a surface is easy, and its charge, thus, strongly depends on solution pH. For the silica surface, on the other hand, most sites are neutral (protonated group), and only very few are charged (deprotonated group). To charge up such a surface is more difficult, and its charge hardly depends on solution pH at low charge densities.

Within the CR approximation, each surface is characterized only by two basic parameters, namely, the diffuse layer potential $\psi^{D,\infty}$ and the regulation parameter p . Both parameters are properties of a *single* isolated surface and only depend on the solution composition (e.g., salt concentration, pH). Once these parameters are known, the properties of *two* interacting surfaces can be calculated. This idea simplifies the description of interacting surfaces enormously, be it in symmetric or asymmetric situations. In the latter case, the two basic parameters must be specified for each individual surface and will be of course different.

While the evaluation of the complete charge–potential relationship for the surface is somewhat tedious in the present examples, it is nevertheless straightforward. Charge–potential relationships can be also obtained from more complicated models of the surface dissociation behavior. In many situations,

however, models of the surface dissociation behavior are not available, and the charge–potential relationship cannot be evaluated. In such situations, the regulation behavior cannot be treated rigorously. However, the regulation behavior can still be discussed within the CR approximation for such a surface.

4. Forces in Symmetric Systems

Let us first demonstrate the usefulness of the CR approximation in symmetric systems. We shall consider two cases, one at low ionic strength, where we expect behavior resembling PB, and the other one at higher ionic strength resembling CC.

To be specific, let us focus on the interaction between two identical rutile surfaces at pH 3.8 and an ionic strength of 1 mM. The results are shown in Figure 3. The corresponding surface charge densities, diffuse layer potentials, and regulation parameters for the isolated surface are summarized in Table 2 and indicated in Figure 2 with markers.

Consider first the variation of the surface charge density and of the diffuse layer potential upon approach (see Figure 3a,b). One observes that the charge density decreases substantially, while the potential increases only marginally. At contact, the charge density vanishes, and the surface potential attains a value of 118 mV, which is close to the value of 111 mV for the isolated surface. The behavior is indeed not too different from the CP conditions, which is also indicated by the low value of the regulation parameter $p \approx 0.191$. When this parameter is

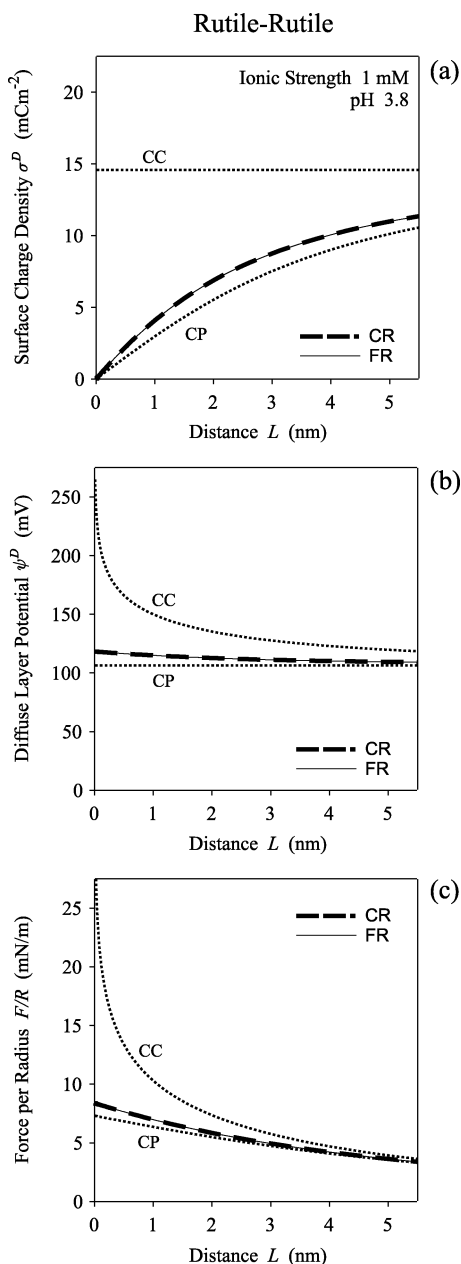


Figure 3. Interaction of two rutile surfaces as a function of separation at pH 3.8 and an ionic strength of 1 mM. Results of the full regulation (FR) calculation are compared with those of the CR approximation. The limits of CC and CP are indicated. For this symmetric system we show (a) surface charge density, (b) diffuse layer potential, and (c) force per unit curvature radius.

TABLE 2: Diffuse Layer Potentials and Regulation Parameters for the Systems Considered^a

	figure	pH	$\psi_1^{D,\infty}$ (mV)	p_1	$\psi_2^{D,\infty}$ (mV)	p_2
rutile–rutile	3	3.8	+106	0.191	+106	0.191
	4	3.8 ^b	+67.0	0.536	+67.0	0.536
rutile–goethite	5a	3.8	+106	0.191	+214	0.706
	5b	5.0	+44.4	0.075	+190	0.598
	5c	6.3	−27.8	0.063	+152	0.418
rutile–silica	6a	5.0	+44.4	0.075	−22.3	0.556
	6b	6.3	−27.8	0.063	−64.5	0.390
	6c	8.0	−116	0.220	−126	0.399

^a Ionic strength is 1 mM, except in case *b* where it is 100 mM.

used in the CR boundary condition, the results for the charge density and the potential are indistinguishable on the scale of the graph from the results obtained by the full regulation

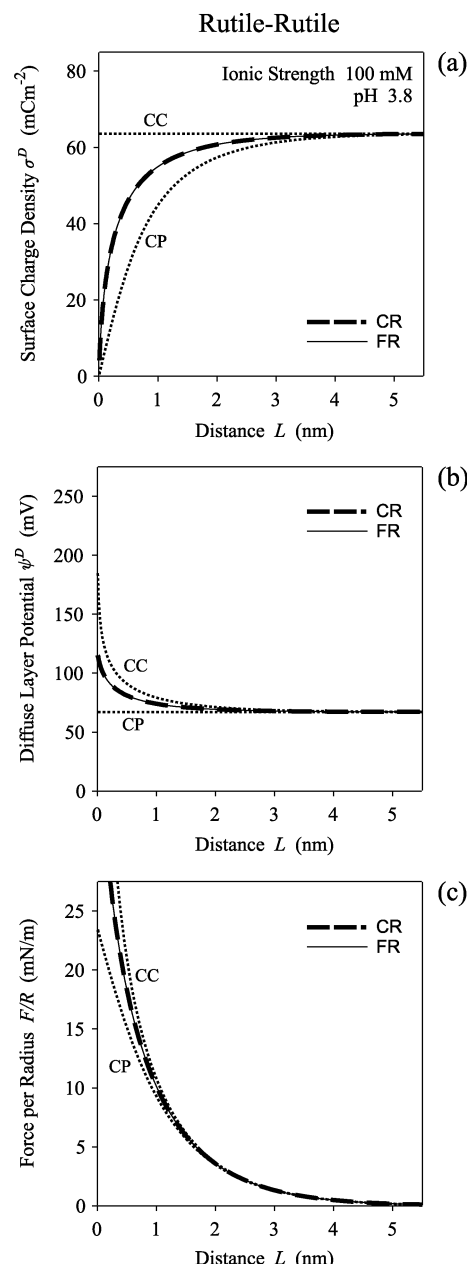


Figure 4. Interaction of two rutile surfaces as a function of separation at pH 3.8 at an ionic strength of 100 mM. Results of the full regulation (FR) calculation are compared with those of the CR approximation. The limits of CC and CP are indicated. For this symmetric system we show (a) surface charge density, (b) diffuse layer potential, and (c) force per unit curvature radius.

calculation. The latter uses the basic Stern model described above.

The interaction forces are repulsive and governed by double layer overlap (see Figure 3c). The CR approximation yields basically an identical result as the full regulation calculation. The resulting force is relatively close to the result for CP boundary conditions and far away from the CC case.

Figure 4 illustrates the analogous results at an ionic strength of 100 mM. The relevant parameters are summarized in Table 2. The regulation parameter $p \approx 0.536$ is situated closer to the CC condition. With decreasing distance, one observes that the charge density remains relatively constant at larger distances but decreases rapidly near contact. At the same time, the surface potential increases substantially. At contact, the surfaces are neutral and attain a potential of 115 mV, while for the isolated

surface one has 67 mV. This pronounced change in the surface potential leads to a force which lies closer to the CC condition. The distance dependence is again accurately captured by the CR approximation.

To conclude our discussion on the symmetric system, let us compare the results with a superposition approximation for the regulating case suggested earlier.³² These authors have proposed to approximate the force in the regulating case by a linear superposition of the CP and CC force obtained from the PB equation weighted with the regulation parameter p . This result is asymptotically exact on the PB level for large distances and coincides with the CR approximation in this regime. On the other hand, the superposition approximation fails near contact, while the CR approximation can be exact in this regime, provided the charging curve of the inner layer is a linear function of the potential. Thus, the present CR approximation is similar in spirit to the superposition approximation but more accurate in practice. The computational effort is the same in both cases.

5. Forces in Asymmetric Systems

The main advantage of the CR boundary condition consists of the simplicity it offers to treat asymmetric systems. While effects of charge regulation are much more important in asymmetric than in symmetric systems, the only way to describe these systems so far was to explicitly include all relevant chemical equilibria on both surfaces.^{29,30,33} Needless to say, such calculations are cumbersome and highly model-dependent. Moreover, an equilibrium model for the surface is not available in many situations.

The CR condition packs the entire surface chemistry into two parameters, namely, the diffuse layer potential and the regulation parameter. For an asymmetric system, one naturally has to consider these two parameters for each surface, thus, dealing with four parameters $\psi_1^{D,\infty}$ and p_1 for surface 1 and $\psi_2^{D,\infty}$ and p_2 for surface 2. The CR condition represents a natural extension of the existing charge regulation treatment on the linearized Debye–Hückel level³⁷ to the nonlinear PB regime. For low surface potentials, both approaches coincide.

As the first asymmetric example, let us consider the forces between a rutile and a goethite surface at an ionic strength of 1 mM as a function of pH. Note that the PZC of rutile lies below the PZC of goethite. For this reason, the forces at large distances will be repulsive at low pH, attractive at intermediate pH, and again repulsive at high pH. Figure 5 summarizes some of the important cases in the transition from the repulsive to the attractive regime. Because this transition is somewhat complex, let us first discuss the dependence of the forces and then the quality of the CR approximation.

At very low pH, both surfaces are highly charged, strongly repulsive, and resemble the behavior in the symmetric system. With increasing pH, the force becomes progressively attractive near contact, and the force profile develops a characteristic maximum. Such a situation is encountered at pH 3.8 (see Figure 5a). The force is repulsive at large distances but decreases at small distances. This behavior differs strongly from the fully repulsive CC case but resembles the CP case, where a maximum in the force is observed at larger separations. Upon approach, the highly charged goethite surface maintains its surface charge and surface potential, but the surface charge of rutile becomes negative, while the surface potential remains positive. This charge reversal is the origin of the weaker repulsion near contact.

With increasing pH, the force at small separations decreases continuously and eventually becomes attractive. For example,

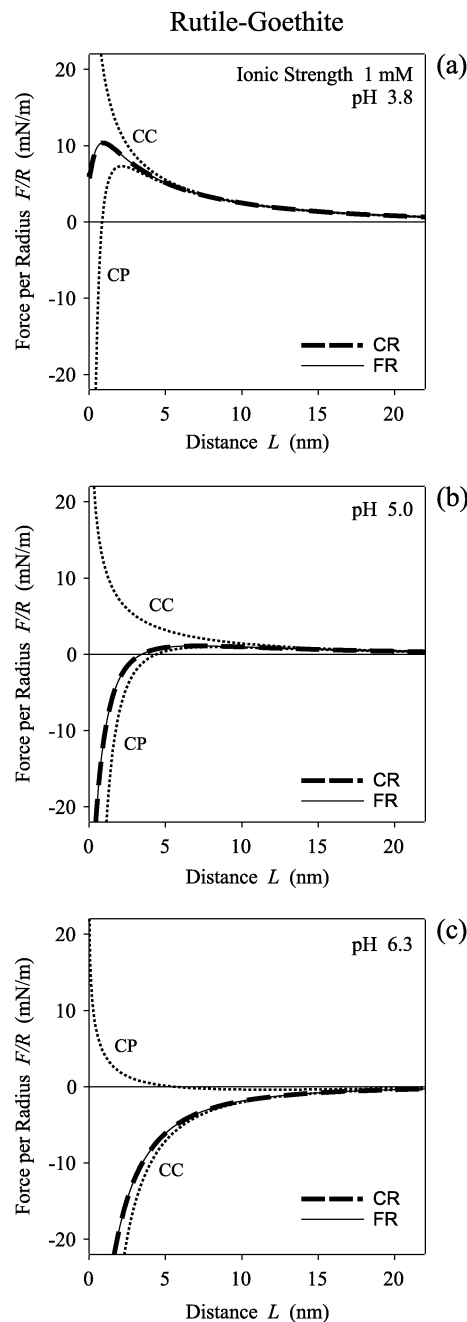


Figure 5. Interaction of a rutile and an iron oxide surface as a function of separation at an ionic strength of 1 mM. Results of the full regulation (FR) calculation are compared with those of the CR approximation. The limits of CC and CP are indicated. For this asymmetric system we show the force per unit curvature radius for pH values of (a) 3.8, (b) 5.0, and (c) 6.3.

this situation occurs at pH 5.0 (see Figure 5b). Because both surfaces are still positively charged, the force remains repulsive at large separations. At smaller separations, the force becomes attractive as a result of a similar charge reversal mechanism as discussed above. At this point, however, the surface potential of the goethite surface decreases upon approach, while its surface charge increases.

With further increase of the pH, rutile goes through the PZC, and its charge becomes negative. This surface will be attracted to a positively charged iron oxide surface. This case is encountered at pH 6.3 (see Figure 5c). The attraction persists down to contact, and the behavior starts to resemble the CC case. Increasing the pH further, the forces become repulsive

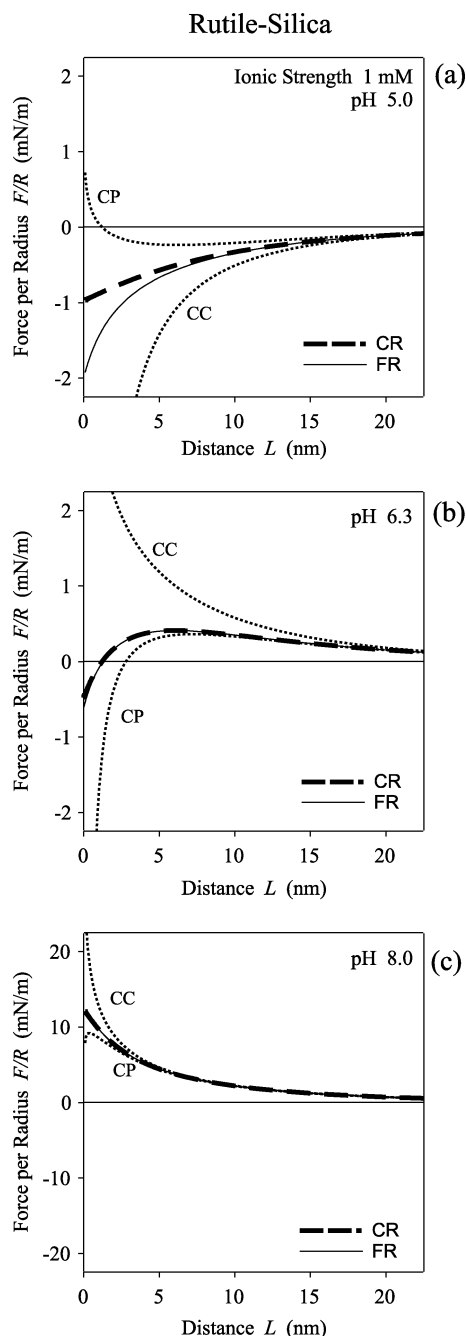


Figure 6. Interaction of a rutile and a silica surface as a function of separation at an ionic strength of 1 mM. Results of the full regulation (FR) calculation are compared with those of the CR approximation. The limits of CC and CP are indicated. For this asymmetric system we show the force per unit curvature radius for pH values of (a) 5.0, (b) 6.3, and (c) 8.0.

along a similar scenario. In any case, the CR approximates the results based on full regulation extremely well.

As a second example of an asymmetric system, consider the interaction forces between rutile and silica, again at an ionic strength of 1 mM. In contrast to the previous situation, silica always remains negative, which means that the forces at large distances will be attractive at low pH and repulsive at high pH. Figure 6 summarizes the results. Again we first discuss the dependence of the forces and then discuss the quality of the CR approximation.

At low pH, the silica surface is basically neutral, which leads to weak interaction forces and strong charge regulation effects. This situation is encountered at pH 5.0 (see Figure 6a). One

observes a weak attractive force, which lies between the CP and the CC cases. The rutile surface behaves similarly to a CP surface, while the surface charge of the silica surface decreases and its potential increases and becomes positive.

At higher pH, the surface charge of rutile changes its sign and the force becomes repulsive at large distances. One finds this case at pH 6.3 (see Figure 6b). As a result of regulation effects, however, the force becomes attractive close to contact. With decreasing separation, the surface charge of rutile increases, while the surface potential decreases. The surface charge of silica increases at first but starts to decrease at shorter distances. This nonmonotonic behavior leads to the attractive force at smaller separations. At even higher pH values, negative charge builds up on both surfaces, and the system again resembles the symmetric case. This situation is found at pH 8 (see Figure 6c).

The CR approximation works again very well, but with one important exception. As can be seen in Figure 6a, the results for full regulation are in substantial disagreement with the CR approximation near contact. This possibility was already invoked above; see Figure 1b. The intrinsic surface charge density of silica vanishes asymptotically with increasing diffuse layer potential, and the approximation of this function by a straight line is insufficient near contact. At larger distances, the CR approximation works well, as it should.

At higher pH, on the other hand, the CR approximation is accurate again despite the strongly nonlinear character of the charge–potential relationship for the surface. We, therefore, suspect, that situations where the CR approximation fails are infrequent, and the gain in simplicity largely outweighs this minor disadvantage.

6. Conclusions

The CR approximation provides an accurate description of the interaction forces of ionizable surfaces across an electrolyte solution on the PB level. The spirit of the approximation is to linearize the charge–potential relationship of the surface around the potential of the isolated surface but otherwise to solve the PB equation for the diffuse layer exactly. This approximation eliminates the need to treat the interacting surfaces simultaneously with the chemical adsorption equilibria of charged species to each surface. In fact, no mathematical model for the ionization of the surface is necessary, and the entire chemical response of the surface is expressed in terms of two parameters, namely, the diffuse layer potential $\psi^{D,\infty}$ and the regulation parameter p . Both parameters refer to an isolated surface only and, thus, can also be obtained from classical surface equilibrium models or by probing the interfaces by surface-sensitive techniques (i.e., electrokinetic measurements).

The classical boundary condition of CP corresponds to $p = 0$ and that of CC corresponds to $p = 1$. In the general case, the regulation parameter p typically assumes values in between. This parameter can be related to two capacitances, the diffuse layer capacitance C^D and the inner layer capacitance C^I (cf. eq 12). When the inner layer charge remains constant, the inner layer capacitance is larger than the diffuse layer capacitance, and the surface behaves CC-like ($p = 1$). When the inner layer charge can be easily regulated by adsorption of charged species, the inner capacitance is small, and the surface behaves CP-like ($p = 0$). The diffuse layer capacitance increases with increasing magnitude of the surface potential and with increasing ionic strength. As a consequence, the regulation parameter will show a similar dependence.

The CR approximation represents a natural generalization of the linearized theory of Carnie and Chan.³⁷ The latter theory is

based on the linear Debye–Hückel equation and is, thus, of rather limited validity in practice. By treating the PB equation exactly and linearizing the charge–potential relationship around the state of the isolated surface, we retain the simplicity of the Carnie and Chan approach³⁷ but are able to substantially extend its range of validity. On the basis of our experience so far, the approximation is excellent in most practical situations even at small separations, in symmetric as well as in asymmetric systems. Several successful examples have been presented here.

In some cases, however, the CR approximation might become poor at small separations. One important case concerns a nearly neutral surface, to which only traces of the charge-determining ions are adsorbed. In this situation, the charging curve of the inner layer approaches asymptotically 0 for high potentials, and the CR approximation might produce unsatisfactory results near contact. Nevertheless, we suspect that these situations are probably of minor importance in practice, and for this reason we expect that the CR approximation will provide a most useful framework to discuss electrostatic interactions between charged surfaces.

Acknowledgment. This work was supported by the Swiss National Science Foundation, Swiss Commission of Technology and Innovation, and the BASF Aktiengesellschaft.

References and Notes

- (1) Israelachvili, J. *Intermolecular and Surface Forces*; Academic Press: London, 1991.
- (2) Vigil, G.; Xu, Z.; Steinberg, S. *J. Colloid Interface Sci.* **1996**, *165*, 367.
- (3) Xu, Z.; Ducker, W.; Israelachvili, J. *Langmuir* **1996**, *12*, 2263.
- (4) Frechette, J.; Vanderlick, T. K. *Langmuir* **2001**, *17*, 7620.
- (5) Poptoshev, E.; Rutland, M. W.; Claesson, P. M. *Langmuir* **2000**, *16*, 1987.
- (6) Ducker, W. A.; Senden, T. J.; Pashley, R. M. *Nature* **1991**, *353*, 239.
- (7) Ducker, W. A.; Senden, T. J.; Pashley, R. M. *Langmuir* **1992**, *8*, 1831.
- (8) Butt, H. J. *Biophys. J.* **1991**, *60*, 1438.
- (9) Hartley, P. G.; Larson, I.; Scales, P. J. *Langmuir* **1997**, *13*, 2207.
- (10) Toikka, G.; Hayes, R. A.; Ralston, J. *Langmuir* **1996**, *12*, 3783.
- (11) Toikka, G.; Hayes, R. A. *J. Colloid Interface Sci.* **1997**, *191*, 102.
- (12) Giesbers, M.; Kleijn, J. M.; Cohen Stuart, M. A. *J. Colloid Interface Sci.* **2002**, *252*, 138.
- (13) Pagac, E. S.; Tilton, R. D.; Prieve, D. C. *Langmuir* **1998**, *14*, 5106.
- (14) Bevan, M. A.; Prieve, D. C. *Langmuir* **1999**, *15*, 7925–7936.
- (15) Hoek, E. M. V.; Bhattacharjee, S.; Elimelech, M. *Langmuir* **2003**, *19*, 4836.
- (16) Stahlberg, J.; Jonsson, B. *Anal. Chem.* **1996**, *68*, 1536.
- (17) Zheng, J.; Behrens, S. H.; Borkovec, M.; Powers, S. E. *Environ. Sci. Technol.* **2001**, *35*, 2207.
- (18) Derjaguin, B. V.; Landau, L. *Acta Physicochim. URSS* **1941**, *14*, 633.
- (19) Verwey, E. J. W.; Overbeek, J. T. G. *Theory of the Stability of Lyophobic Colloids*; Elsevier: Amsterdam, 1948.
- (20) Bostrom, M.; Williams, D. R. M.; Ninham, B. W. *Phys. Rev. Lett.* **2001**, *87*, 168103.
- (21) Guldbrand, L.; Jönsson, B.; Wennerström, H.; Linse, P. *J. Chem. Phys.* **1984**, *80*, 2221.
- (22) Kjellander, R.; Greberg, H. *J. Electroanal. Chem.* **1998**, *450*, 233.
- (23) Kjellander, R.; Åkerson, T.; Jönsson, B.; Marčelja, S. *J. Chem. Phys.* **1992**, *97*, 1424.
- (24) Levin, Y. *Rep. Prog. Phys.* **2002**, *65*, 1577.
- (25) Frens, G.; Overbeek, J. T. G. *J. Colloid Interface Sci.* **1972**, *38*, 376.
- (26) Biesheuvel, P. M. *Langmuir* **2002**, *18*, 5566.
- (27) Hillier, A. C.; Kim, S.; Bard, A. J. *J. Phys. Chem.* **1996**, *100*, 18808.
- (28) Barten, D.; Kleijn, J. M.; Duval, J.; van Leeuwen, H. P.; Lyklema, J.; Cohen Stuart, M. A. *Langmuir* **2003**, *19*, 1133.
- (29) McCormack, D.; Carnie, S. L.; Chan, D. Y. C. **1995**, *169*, 177.
- (30) Biesheuvel, P. M. *J. Colloid Interface Sci.* **2004**, *275*, 514.
- (31) Behrens, S. H.; Borkovec, M. *J. Phys. Chem. B* **1999**, *103*, 2918.
- (32) Behrens, S. H.; Borkovec, M. *J. Chem. Phys.* **1999**, *111*, 382.
- (33) Behrens, S. H.; Borkovec, M. *Phys. Rev. E* **1999**, *60*, 7040.
- (34) Zhmud, B. V.; Meurk, A.; Bergstrom, L. *J. Colloid Interface Sci.* **1998**, *207*, 332.
- (35) Ninham, B. W.; Parsegian, V. A. *J. Theor. Biol.* **1971**, *31*, 405.
- (36) Reiner, E. S.; Radke, C. J. *Adv. Colloid Interface Sci.* **1993**, *47*, 59.
- (37) Carnie, S. L.; Chan, D. Y. C. *J. Colloid Interface Sci.* **1993**, *161*, 260.
- (38) Healy, T. W.; White, L. R. *Adv. Colloid Interface Sci.* **1978**, *9*, 303.
- (39) Westall, J.; Hohl, H. *Adv. Colloid Interface Sci.* **1980**, *12*, 265.
- (40) Hiemstra, T.; de Wit, J. C. M.; van Riemsdijk, W. H. *J. Colloid Interface Sci.* **1989**, *133*, 105.
- (41) Borkovec, M.; Jönsson, B.; Koper, G. J. M. *Surf. Colloid Sci.* **2001**, *16*, 99.
- (42) Numerical Algorithm Group, Fortran Library, Mark 19, Routine D02RAF.